Spectroscopic analysis of A- and F-type stars observed in the *Kepler* field

Magdalena Polińska[1], Ewa Niemczura[2], Simon J. Murphy[3,4], Hans Bruntt[5], Katrien Uytterhoeven[6,7] and Peter De Cat[8]

1. Institute Astronomical Observatory, Adam Mickiewicz University, Słoneczna 36, 60–286 Poznań, Poland
2. Astronomical Institute, University of Wrocław, Kopernika 11, 51–622 Wrocław, Poland
3. Sydney Institute for Astronomy (SIfA), School of Physics, Univeristy of Sydney NSW 2006, Australia
4. Stellar Astrophysics Centre, Department of Physics and Astronomy, Aarhus University, 8000 Aarhus C, Denmark
5. Department of Physics and Astronomy, Stellar Astrophysics Centre, Aarhus University, DK-8000 Aarhus C, Denmark
6. Institutio de Astrofisica de Canarias, E-38205 La Laguna, Tenerife, Spain
7. Universidad de La Laguna, Departamento de Astrofisica, E-38206 La Laguna, Tenerife, Spain
8. Royal observatory of Belgium, Ringlaan 3, B-1180 Brussel, Belgium

We present results obtained from a spectroscopic analysis of high-resolution spectra taken with the ESPADONS spectrograph at the Canada-France-Hawaii Telescope and the SOPHIE spectrograph installed at the telescope in Haute-Provence Observatory. The data were collected for A- and F-type stars observed in the *Kepler* field. The presented sample of stars consists of objects with the projected rotational velocities lower than $60\,\mathrm{km\,s^{-1}}$. The atmospheric parameters, abundances and rotational velocities were calculated using the iSpec code with spectrum synthesis technique.

1 Observations

We analysed high-resolution spectra taken with two spectrographs, ESPADONS attached to the 3.6-m CFHT (Canada-France-Hawaii Telescope) and SOPHIE installed at the 1.93-m telescope in the HPO (Haute-Provence Observatory). The ESPADONS spectra have a resolving power $R \sim 81\,000$ and cover the range from 3700 to 10 500 nm. For the second spectrograph resolving power is $R \sim$75 000 with the wavelength range of 3800–9800 nm. The signal-to-noise (S/N) ratio of the spectra is similar for both spectrographs and it is between 100-150.

2 iSpec code

To estimate atmospheric parameters, we used the iSpec open source code (Blanco-Cuaresma et al., 2014), which offers various kinds of atmospheric models, atomic data, and analysis techniques. We used spectrum synthesis that compares the observed spectra with synthetic ones. To calculate synthetic spectra we made use of the Atlas9 and Synthe codes (Kurucz, 2005), and the line list from the VALD database (Kupka et al., 2011). The solar abundances were taken from Asplund et al. (2009).

3 Balmer Lines and Atmospheric Parameters

The effective temperature $T_{\rm eff}$ was estimated using the following Balmer lines Hα, Hβ, Hγ and Hδ. When the two first Balmer lines were badly normalized we used

KIC number	$T_{\rm eff}$ Balmer [K]	$T_{\rm eff}$ [K]	$\log g$ [dex]	[M/H] [dex]	ξ [km s^{-1}]	$v \sin i$ [km s^{-1}]	A(Fe) [dex]
3733735*	6700±200	6900±90	4.3±0.2	0.00±0.08	1.8±0.1	18±3	7.50±0.06
4931390	6800±100	6800±90	4.3±0.1	-0.10±0.08	1.7±0.1	7±2	7.38±0.10
7180968	6900±200	7070±90	3.5±0.3	0.10±0.22	3.8±0.1	55±1	7.61±0.14
7529180	6600±150	6800±110	4.2±0.2	-0.05±0.10	1.9±0.2	32±2	7.44±0.11
7800289	6300±200	6560±110	3.6±0.2	-0.30±0.07	2.1±0.1	21±1	7.20±0.10
8343931	6500±100	6580±90	3.6±0.1	0.00±0.05	2.1±0.1	54±1	7.48±0.15
8677933	6100±200	5800±100	3.1±0.2	-0.15±0.10	1.9±0.1	50±2	7.36±0.20
9025370	6000±200	5800±100	4.0±0.1	-0.30±0.10	0.0±0.1	7±1	7.02±0.10
9116461	6500±100	6500±90	4.2±0.1	-0.20±0.10	1.5±0.1	17±1	7.32±0.08
9851142	7200±100	7300±90	3.7±0.1	0.25±0.05	3.5±0.2	10±1	7.73±0.12
9965715	6600±200	6400±100	4.1±0.1	-0.25±0.05	1.4±0.1	11±2	7.15±0.07
10010623	6500±200	6600±90	4.0±0.1	0.30±0.05	1.6±0.1	43±1	7.79±0.20
11018874	6300±100	6500±100	4.1±0.2	-0.20±0.10	1.9±0.1	56±2	7.33±0.01
11253226*	6900±100	6800±100	4.1±0.1	-0.15±0.05	1.8±0.1	15±1	7.35±0.05
11498538	6500±200	6760±100	3.6±0.2	0.05±0.06	2.5±0.1	41±2	7.55±0.25
11708170*	6700±200	6950±130	3.8±0.1	-0.30±0.10	2.3±0.2	39±2	7.18±0.10

Table 1: $T_{\rm eff}$ derived from the Balmer lines (column 2) and the atmospheric parameters obtained from spectrum synthesis (columns 3-8) for the analysed stars (column 1). The stars marked with an asterisk were observed with the SOPHIE spectrograph.

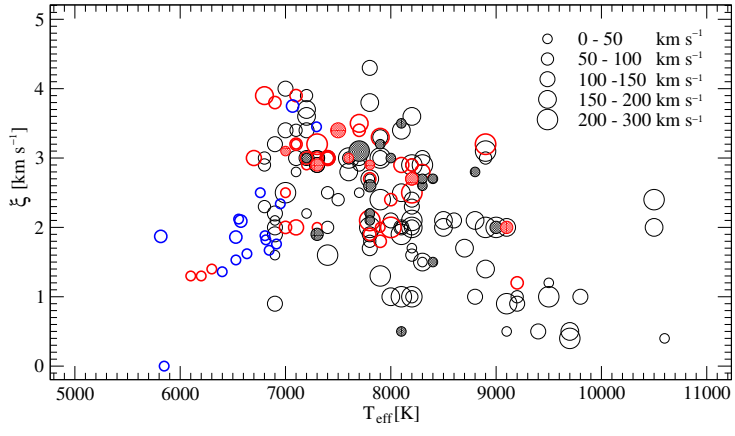

Fig. 1: The microturbulent velocities ξ as a function of $T_{\rm eff}$. Stars from the current work are marked with blue circles, data from Paper I (Niemczura et al., 2015) and II (Niemczura et al., 2017) are shown as black and red circles, respectively. Chemically peculiar (CP) stars (from Paper I and II) are marked with filled circles. The size of circles is correlated to $v \sin i$ (see legend at the top right corner).

only Hβ and Hα lines. For stars with $T_{\rm eff} < 8000$ K, Balmer lines are not sensitive to surface gravity $\log g$ (Smalley, 2005), so this value was fixed to 4.0 dex during calculation. To estimate the uncertainty of $T_{\rm eff}$, we checked the differences in the determined $T_{\rm eff}$ values from separate Balmer lines. These types of error are mainly due to bad normalisation. All the obtained values with their errors are listed in Tab. 1.

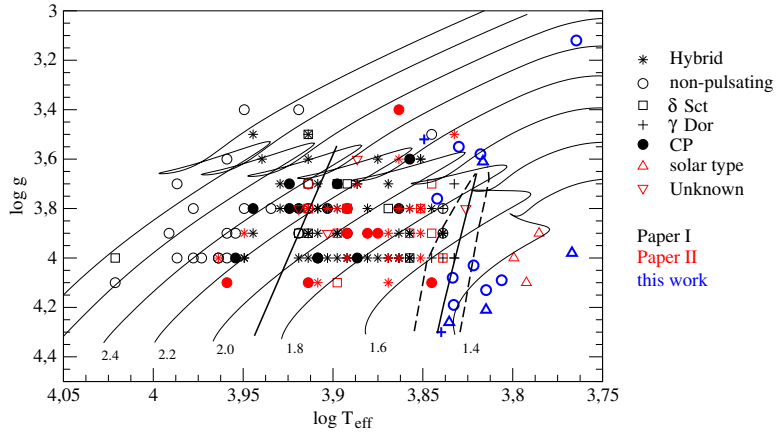

Fig. 2: The $\log g$ – $\log T_{\rm eff}$ diagram for the stars analysed in this work and Paper I and II. Different kind of pulsating and CP stars are marked with different symbols (see legend on the right). Evolutionary tracks were calculated with Time Dependent Convection (Grigahcène et al., 2005). The instability stripes for δ Scuti and γ Doradus stars are overplotted with full and dashed lines, respectively (Murphy et al., 2015).

The atmospheric parameters ($T_{\rm eff}$, $\log g$, metallicity [M/H], microturbulent velocity, ξ, and the projected rotational velocity, $v \sin i$, were calculated using spectrum synthesis technique. At first, we chose segments for which the synthetic spectra were computed, avoiding regions contaminated by telluric lines. In the next step, the Fe I and Fe II lines were analysed. For the iteration process, $T_{\rm eff}$, $\log g$, [M/H], ξ, and $v \sin i$ were considered as free initial parameters. During calculation, we assumed the macroturbulence to be equal to zero. The iron abundances A(Fe) were also calculated. All results of the fitting procedure are presented in Fig. 1. The iSpec code estimates the uncertainties from the covariance matrix built with the nonlinear least-squares fitting algorithm. These estimations depend on the flux errors which can be added to the observed flux from the calculation of the S/N. The uncertainties of the iron abundances A(Fe) were calculated using the standard deviation of the sample.

4 Summary

We presented the analysis of spectra of A- and F-type stars observed in the *Kepler* field. Our sample of stars consists of objects with $v \sin i < 60\,{\rm km\,s^{-1}}$. The stars analysed in this work are part of the project for which data were already published in Paper I (Niemczura et al., 2015) and Paper II (Niemczura et al., 2017) of this series. The results derived from our spectral analysis are consistent with those from previous determinations for A- and F-type stars. In Fig. 2, we visualized the location of these stars with respect to evolutionary tracks and the instability strips for δ Scuti and γ Doradus stars.

Acknowledgements. This work was supported by the Polish National Science Centre through grant No. 2014/13/B/ST9/00902.

References

Asplund, M., Grevesse, A. J., Nand Sauval, et al., *ARA&A* **47**, 481 (2009)
Blanco-Cuaresma, S., Soubiran, C., Heiter, U., et al., *A&A* **569**, A111 (2014)
Grigahcène, A., Dupret, M. A., Gabriel, M., et al., *A&A* **434**, 1055 (2005)
Kupka, F., Dubernet, M. L., VAMDC-Collaboration, *Balt.Astron* **20**, 503 (2011)
Kurucz, R. L., *Mem. Soc.Astron.It.Supp.* **8**, 14 (2005)
Murphy, S. J., Bedding, T. R., Niemczura, E., et al., *MNRAS* **447**, 3948 (2015)
Niemczura, E., Murphy, S. J., Smalley, B., et al., *MNRAS* **450**, 2764 (2015)
Niemczura, E., Polińska, M., Murphy, S. J., et al., *MNRAS* **470**, 2870 (2017)
Smalley, B., *MSAIS* **8**, 130 (2005)